ADVANCES OF BLOOD VESSEL MORPHOLOGY ANALYSIS IN 3D MAGNETIC RESONANCE IMAGES [1]

Maciej Orkisz, Marcela Hernández-Hoyos, Philippe Douek, Isabelle Magnin

CREATIS, CNRS Research Unit (UMR 5515), affiliated to INSERM, Lyon, France
CREATIS INSA 502, 69621 Villeurbanne cedex, France, maciej.orkisz@creatis.insa-lyon.fr

Abstract We deal with image processing applied to three-dimensional (3D) analysis of vascular morphology in magnetic resonance angiography (MRA) images. It is, above all, a state-of-the-art survey. Both filtering and segmentation techniques are discussed. We briefly describe our most recent contribution : an anisotropic non-linear filter which improves visualization of small blood vessels. Enhancement of small vessels is obtained by combining a directional L-filter applied according to the locally estimated orientation of image content and a 2D Laplacian orthogonal to this orientation.

Key words: 3D image processing, medical imaging, magnetic resonance angiography, image enhancement, image segmentation

1. Introduction

Our work is motivated by diagnosis, treatment planning and follow-up of arterial diseases. Atherosclerosis is the principal acquired affection of the arterial wall. Its consequences depend on its localization and on the size of the vessel. They are of two natures : arterial lumen obstruction (stenosis) and arterial wall vulnerability which may lead to excrescence (aneurysm) and rupture. Diagnosis of these pathologies is greatly aided by imaging techniques. There are several challenges concerning angiography images. They obviously should clearly display the pathological artery segment. In the case of severe obstructions, the physician also needs to assess the collateral vascularization, *i.e.* to see a network of thin vessels around the diseased region. Qualitative assessment is usually done in two-dimensional (2D) projection images. However, the choice and planning of pharmacological, intra-vascular or surgical treatment depend on precise measurements such as length, different diameters and section areas of the diseased segment. These quantitative measurements should take full advantage of 3D information. The latter requirement, as well as the invasive character of the conventional 2D X-ray digital subtraction angiography (DSA), are the reasons for which 3D imaging techniques such as MRA and spiral computed tomography (CT) tend to replace DSA.

Like the medical objectives, image processing challenges are twofold : 1) vessel enhancement and noise removal to improve the qualitative analysis, 2) 3D segmentation and quantification for the sake of (semi-)automated measurements. Both tasks are difficult, due to the specificity of the data. Questions how to enhance thin vessels and not to amplify noise, how to remove

[1] This work is in the scope of the scientific topics of the PRC-GDR ISIS research group of the French National Center for Scientific Research (CNRS).

noise and not to wipe out thin vessels, are still an issue. Similarly, most segmentation techniques are designed for large and homogenous regions, while many blood vessels are not thicker than 3 pixels, their structure is complex, with ramifications, and their intensity is often relatively heterogeneous, due to partial volume effect, flow artifacts and other effects. In section 2, an outline of the state of the art of the angiography image processing shall be given. In section 3, our contribution in vessel enhancement field shall be presented.

2. State of the art

There is a rich literature about 2D DSA image enhancement and segmentation methods. Many of them could be extended to 3D, but computational cost of these extensions would often be prohibitive. Although some of these methods shall be cited hereafter, we will focus on the techniques developed specifically for 3D MRA.

2.1. Filtering

We subdivide the filtering techniques into two categories : 1) techniques which try to eliminate noise while conserving vessels, 2) techniques which try to enhance vessels while avoiding noise amplification.

2.1.1. Smoothing

Isotropic low-pass filtering removes noise as well as thin vessels and hence is unsuited for vascular images. Several authors proposed an anisotropic approach where local orientation of structures is first estimated and filtering is locally done along this orientation so as to preserve small vessels and not to blur boundaries of larger structures. This approach implies a two-stage processing (1. orientation estimation, 2. filtering) and there are many possible combinations of methods used at each stage. In [9], smoothing was carried out by anisotropic diffusion in the direction of the least principal curvature. One of the methods proposed in [2] applied a morphological operation of crest detection, using directional (linear) tools, and selected the direction giving the strongest response. Another one selected the local orientation from a set of discrete orientations (sticks), by choosing the stick with the smallest intensity variance. In [14] a more robust criterion was proposed, which combined homogeneity within the stick on the one hand and intensity difference between the neighboring sticks on the other hand. In both cases, the median filter was then applied within the selected stick. In [7], the local orientation was estimated using six 3D filters in quadrature. A low-pass filter was then applied in the estimated direction for the purpose of smoothing, while a high-pass filter was applied orthogonally to this direction for the purpose of enhancement.

2.1.2. Enhancement

Smoothed images are less noisy, than the original ones, but thin vessels often remain hardly visible, because their initial intensities are low. To enhance them, each point's intensity can be

replaced by a parameter reflecting the anisotropy of the point's neighborhood. One feature of the vessels is their continuity : image intensity and local orientation vary slowly along the vessel. Starting from each point, a path having this property can be sought, and the parameter can be set equal to the path length [10]. Designed for 2D DSA images, this algorithm would however be too time consuming in 3D.

There were several attempts to characterize the anisotropic properties of the vascular images by non-linear combinations of outputs of directional filters. In [4], a set of directional mean-filters was used. The difference between the strongest and the weakest response was used as anisotropy measure. Indeed, the mean intensity along a vessel should be larger than in perpendicular directions. Directional derivatives can also be exploited. They should be close to zero when calculated along a vessel, and should have large absolute values in orthogonal directions. Various combinations of such filters were proposed in [5] [6].

Directional second derivatives can also be brought together in a Hessian matrix, so as to exploit the matrix's eigenvectors and eigenvalues λ_1, λ_2, λ_3. Indeed, tubular structures should give rise to $\lambda_1 \approx 0$ (the associated eigenvector is tangential to the vessel axis) and to $|\lambda_2| >> |\lambda_1|$, $\lambda_2 \approx \lambda_3$ (the associated eigenvectors lie within the plane locally orthogonal to the vessel). Different combinations of these eigenvalues were proposed to enhance points likely to belong to vessels. Moreover, if appropriately designed and applied at multiple scales, such combinations should give the strongest response at one particular scale corresponding to the vessel caliber [16], [13], [19]. Similar geometrical considerations concerning the principal curvatures led to the use of the Weingarten matrix eigenvalues [11], [15]. However, a common problem of the methods based on derivatives is their noise-sensitivity.

2.2. Segmentation

In spite of the advances in the image processing field, interactive thresholding is still the unique segmentation tool used in the commercial medical image processing software packages! However, several automated algorithms were developed in research laboratories to improve segmentation reproducibility. Three principal approaches can be cited : automatic adaptive thresholding, region-growing and vessel-tracking.

2.2.1. Adaptive thresholding

Usually an adaptive threshold is global and is based on image intensity histogram. In [3] the threshold was calculated iteratively, starting from the image mean value μ_0 plus two standard deviations σ_0. At each iteration, μ_i and σ_i were recalculated after eliminating non-isolated voxels above the current threshold. In [18] and [22], prior knowledge of the actual image acquisition protocol was used to choose intensity distribution model and to deduce the threshold from the histogram, by identifying the model's parameters. Uniform distribution of vessel intensities was assumed. The threshold was set at the intersection between this distribution and the background tissues distribution. The latter was modeled by Gaussians in

time-of-flight (TOF) MRA and by a Rician in phase-contrast (PC) MRA. In [20], the authors also argued that the threshold should depend on the actual image acquisition protocol. They suggested setting the threshold at 50% of the maximum vessel signal in the TOF MRA and contrast-enhanced (CE) MRA, and at 10% in the PC MRA.

2.2.2. Seeded region-growing

Region-growing algorithms require an initial seed selection which usually is manual in medical applications. New voxels are then agglomerated to the current region as far as they satisfy a homogeneity criterion. The criterion often is an intensity threshold. The threshold may vary along the vessel to adapt itself to local intensity statistics. In [1], the threshold was set equal to $max\ (\mu_b+2\sigma_b, \mu_v-2\sigma_v)$, where μ_v, σ_v and μ_b, σ_b respectively were the intensity mean values and standard deviations for voxels already classified as belonging to a vessel and for the remaining ones within a small volume around a current voxel. In [26], the region-growing of both vessel and background was carried out by competition, using two criteria based on the histograms of intensity gradient and of maximum principal curvature. A directional region-growing was proposed in [10]. Local orientations were first estimated for each pixel, by seeking the discrete orientation maximizing the mean intensity within the corresponding stick. New pixels were then agglomerated as far as their orientation agreed with the seed's local orientation. A very interesting method for automated selection of seeds was recently proposed in [27]. It exploits the depth map constructed during maximum intensity projection (MIP). This map, considered as an image, is continuous within regions corresponding to the vessels and presents strong discontinuities elsewhere. A continuity measure calculated in this image is used to segment the 2D MIP image. Since depth of thus obtained regions is known, they are used as seeds in 3D.

2.2.3. Vessel-tracking

The vessel-tracking algorithms in 3D images use (often implicitly) a generalized-cylinder model, *i.e.* an association of an axis (centerline) and a surface (vessel wall). Two approaches can be distinguished. The first one begins by the centerline extraction, then the vessel wall is sought. In [11] [15] the centerline was obtained by chaining local maxima of the principal curvature and no attempt was done to estimate the vessel wall position. An improved continuity of the axis and its reduced noise-sensitivity was obtained in [23][24] using a B-spline curve (snake). An energy function was designed to attract the snake towards local maxima of an anisotropy measure based on the Hessian matrix eigenvalues. A B-spline approximation (active surface) was also used for the vessel wall. The corresponding energy was minimum when the surface was close to isosurface corresponding to an acquisition protocol dependent threshold. In [25], the axis was extracted using inertia moments. The actual vessel boundaries were not extracted. Instead, an estimate of the vessel radius along the axis was deduced from the inertia moments.

In the second approach, named "virtual catheter", axis and boundaries are interdependent. At each step, contours are sought in the plane orthogonal to the current axis orientation, the axis position is re-estimated, the centerline is extended according to the corrected orientation, and so on. In [8], the boundary points were sought radially starting from the current axis position and taking into account the neighboring radii. The axis position was then corrected using the contour's gravity center and the centerline was extended linearly. In [12], linear extension was replaced by a B-spline approximation and the contour detection took into account the neighboring slices to improve continuity. In [17], the local axis orientation was updated in a more complex manner, using intersections between the vessel and eight straight lines equally spaced around the axis and parallel to its current orientation. For the boundary detection in the plane orthogonal to the axis, the authors suggested the use of active contours. Active contours were also used in [13] for the same purpose. In [21], the boundaries were sought more roughly, using a radial search of gradient maxima, starting from different candidate points. The lengths of thus obtained radii were used to calculate a confidence coefficient for each starting point and to select the point which was the likeliest to lie on the centerline. In [28], the boundary search was improved. To obtain a closed contour in the initial coordinates the algorithm sought the minimum cost path in polar coordinates, *i.e.* a line as straight and as vertical as possible, passing through the points with the most negative gradient values.

3. Our contribution

We have already published our contribution in both fields : anisotropic non-linear smoothing [14] and vessel-tracking [25]. Here we propose an operator designed to enhance small vessels while limiting noise amplification. To this purpose we re-use the orientation estimation technique described in [14] and our new operator replaces the median filter used in the smoothing context. Let us briefly recall how the local orientation is estimated. It is selected from a set of discrete orientations represented by "sticks". For the voxels located within vessels, the "best-oriented" stick should locally be parallel to the vessel axis and it should be (almost) entirely included either in the vessel or in the background, to ensure a good homogeneity of the intensity within the stick. Consequently, some of the neighboring sticks parallel to the central stick should belong to the same region as the central stick while the other ones should be located outside this region. Hence the intensity within each of these neighboring sticks should also be homogenous, but there should be a large intensity difference between the central stick and the neighboring sticks lying outside the region it belongs to. Let $\mathbf{S}_i = \{S_i^j : j = 0,1,\ldots,n\}$ be a set of n+1 parallel neighboring sticks for the i-th orientation, where S_i^0 is the central stick. Let σ_i^j be the intensity standard deviation for S_i^j and let g_i^j be the directional mean gradient between S_i^j and S_i^0. The averages respectively of σ_i^j (j = 0,1,…,n) and of $|g_i^j|$ (j = 1,…,n), shall be noted $\overline{\sigma}_i$ and $\overline{g}_i$. The best orientation is the one which maximizes the following criterion :

$$HD_i = \overline{g}_i - \alpha\overline{\sigma}_i \qquad (1)$$

which simultaneously takes into account the intensity homogeneity along the sticks (weighted by a coefficient α), and the intensity difference between the central stick and its neighbors. Because of the mixed use of a homogeneity measure and of a difference measure, we called this operator HD-filter.

3.1. Vessel enhancement operator

Knowing the local orientation it is possible to implement an enhancement scheme similar to the one proposed in [7], *i.e.* to apply a kind of low-pass filter along this orientation and a high-pass in the orthogonal plane. In fact, true low-pass filters (mean, Gaussian) give poor results for very thin and tortuous vessels. Instead, we prefer using L-filters. Let us recall that these filters are based on sorting the voxels in the increasing order of intensity : $I_1 \leq \ldots \leq I_L$, where L is the number of voxels (in our case L is the length of the sticks). An L-filter is any linear combination of thus sorted intensities, with coefficients a_k depending on the rank k. When $a_k = 1/(2W+1)$ for $k = k_0 = (L+1)/2$, $k_0 \pm 1, \ldots k_0 \pm W$ and $a_k = 0$ for the remaining ranks, one obtains a truncated mean. Note that $W = 0$ gives the conventional median filter. Let $\{m_{opt}^{\,j} : j = 0,1,\ldots,n\}$ be the truncated mean values for the considered set of sticks $\mathbf{S}_{opt}$, *opt* is the orientation selected by the HD operator. To obtain the enhancement effect we replace the initial intensity of the central voxel in $S_{opt}^{\,0}$ by :

$$f = (n+1)\cdot m_{opt}^{\,0} - (m_{opt}^{\,1} + \ldots + m_{opt}^{\,n}) \qquad (2)$$

It can be interpreted as combining $m_{opt}^{\,0}$ with a 2D Laplacian applied on the truncated mean values. This combination can be weighted. Similarly, W can be tuned to choose a compromise between smoothing and enhancement effect. Figures 1 and 2 were obtained using $W = 0$.

3.2. Results

This new operator was tested on CE MRA images from 9 patients. Such images are obtained by acquiring two data volumes, one before and the other one after intravascular injection of a contrast agent (gadolinium), and by subtracting the latter from the former. Ideally (without motion artifacts) the subtraction should eliminate non-vascular tissues. In practice it also amplifies noise. Due to a high computational cost of the 3D orientation estimation the tests were carried out in 2D for MIP images.

Our method was compared with a conventional isotropic image enhancement technique which consists in adding to the image its Laplacian. In the sequel the latter shall be referred to as isotropic, while our operator shall be called anisotropic. The comparison was both qualitative and quantitative. The qualitative inspection focused on the visibility of small vessels. The quantitative comparison was based on contrast and noise measurements. An automatic vessel tracking applied to user-selected vessel segments allowed us to measure the mean signal inside and outside the vessels, as well as noise standard deviation in the vessels' vicinity. Let us note

that noise level is usually measured in an image region outside the patient's body. This choice is not appropriate in the case of MRA images since the noise level depends on the local signal level. The measurements were performed for 65 arterial segments of different diameters ranging from 1 to 8 pixels and representing different vascular regions : from carotid arteries to lower-limb arteries, including the abdominal aorta and its branchings.

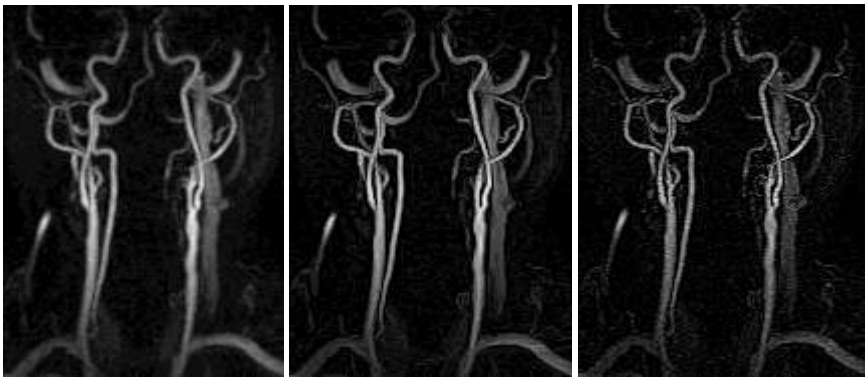

Fig. 1. Images of carotid arteries region : original (left) and enhanced by the anisotropic (middle) and isotropic (right) operator.

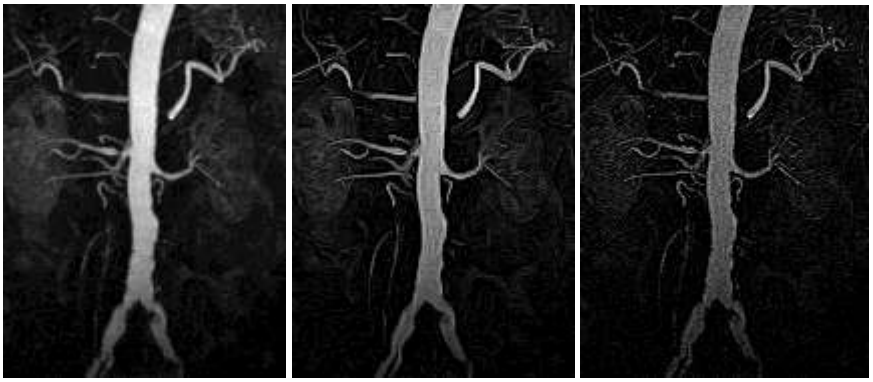

Fig. 2. Images of abdominal aorta, renal and iliac arteries : original (left) and enhanced by the anisotropic (middle) and isotropic (right) operator.

Visual inspection of figures 1 and 2 clearly shows that the arteries appear sharper after application of both the isotropic and anisotropic operators. The conventional isotropic operator however strongly amplifies noise, while our anisotropic operator produces a moderate noise amplification. This qualitative impression was confirmed by the measurements. Indeed, on average our anisotropic operator produced a significant improvement of the contrast (50,5 %)

and a smaller amplification of the noise standard deviation (41,5 %). This resulted in a contrast-to-noise ratio improvement (11,7 %). The isotropic operator produced a similar contrast enhancement (45 %) but noise level was strongly amplified (106,6 %) which led to a contrast-to-noise ratio degradation (-26,3 %).

4. Conclusions

It is very difficult to enhance thin line-like objects and to avoid noise amplification. Our new method using an L-filter applied along the vessels and a Laplacian applied in the plane locally orthogonal to the vessel axis, seems to be a reasonable compromise. It strongly improves the contrast while noise is moderately amplified. This method was successfully applied to magnetic resonance angiography images in which it improved the visualization of small blood vessels. It can therefore be used in practice to aid the assessment of collateral or peripheral vascularization. However, it should not be used as preprocessing before stenosis diagnosis and quantification, because vessel diameters are not necessarily preserved, especially near bifurcations. Future work will focus on the computational cost reduction and on an application of our operator to automated seed detection for the sake of segmentation.

Bibliographic references

1991

[1] Hu X, Alperin N et al, Visualization of MR angiographic data with segmentation and volume-rendering techniques, *J Magn Reson Imaging*, 1, 1991, 539-546.

1992

[2] Vandermeulen D., Delaere D., Suetens P., Bosmans H., Marchal G. : Local filtering and global optimization methods for 3D magnetic resonance angiography (MRA) image enhancement. Proc. SPIE Vol. 1808, Visualization in Biomedical Computing, Chapel Hill NC (USA), 274-288.

1993

[3] Du Y., Parker D.L. et al. : Contrast-to-noise-ratio measurements in three-dimensional magnetic resonance angiography. Invest. Radiol., 28(11), 1004-1009.

1995

[4] Chen H., Hale J. : An algorithm for MR angiography image enhancement. Magn. Reson. in Med., 33, 534-540.

[5] Du Y.P., Parker D.L., Davis W.L. : Vessel enhancement filtering in three-dimensional MR angiography. J. Magn. Reson. Imaging, 5, 151-157.

[6] Du Y.P., Parker D.L. : Digital vessel-enhancement filtering of 3D MR angiograms using long range signal correlation. Int. Soc. Magn. Reson. in Med. Scientific Meeting, Nice (F), 581.

[7] Loock T., Westin C.F. et al. : Multidimensional adaptive filtering of 3D MRA data. Int. Soc. Magn. Reson. in Med. Scientific Meeting, Nice (F), 716.

[8] Verdonck B., Bloch I. et al. : Blood vessel segmentation and visualization in 3D MRA and spiral CT angiography. Comp. Assisted Radiol., Berlin (GER), (Elsevier), 177-182.

1996

[9] Krissian K., Malandain G., Ayache N. : Directional anisotropic diffusion applied to segmentation of vessels in 3D images. INRIA (F) research report # 3064.
[10] Kutka R., Stier S. : Extraction of line properties based on direction fields. IEEE Trans. MI, 15(1), 51-58.
[11] Prinet V., Monga O., Ma S.D. : Extraction of vascular network in 3D images. Int. Conf. Image Processing, Lausanne (CH), 307-310.
[12] Verdonck B., Bloch I. et al. : Accurate segmentation of blood vessels from 3D medical images. Int. Conf. Image Processing, Lausanne (CH), 311-314.

1997

[13] Lorenz C., Carlsen I.C. et al. : Multiscale line segmentation with automatic estimation of width, contrast and tangential direction in 2D and 3D medical images. CVRMed, Grenoble (F), (Springer), 233-242.
[14] Orkisz M., Bresson C. et al. : Improved vessel visualization in MR angiography by non-linear anisotropic filtering. Magn. Reson. in Med., 37, 914-919.
[15] Prinet V., Monga O., Rocchisani J.M. : Vessel representation in 2D and 3D angiograms. Comp. Assisted Radiol., (Elsevier), 240-245.
[16] Sato Y., Nakajima S. et al. : 3-D multiscale line filter for segmentation and visualization of curvilinear structures in medical images. CVRMed, Grenoble (F), (Springer), 213-222.
[17] Swift R.D., Ramaswamy K., Higgins W.E., Adaptive axes-generation algorithm for 3D tubular structures. Int. Conf. Image Processing, Sta Barbara CA (USA), vol. 2, 136-139.
[18] Wilson D.L., Noble J.A., Segmentation of cerebral vessels and aneurysms from MR angiography data. 15th Int. Conf. Information Processing in Med. Imaging, Poultney VT (USA), (Springer), 423-428.

1998

[19] Frangi A.F., Niessen W.J. et al. : Multiscale vessel enhancement filtering. MICCAI, Cambridge MA (USA), 130-137.
[20] Hoogeven R.M., Bakker C.J.G., Viergever M.A. : Limits to the accuracy of vessel diameter measurement in MRA. J. Magn. Reson. Imaging, 8(6), 1228-1235.
[21] Wink O., Niessen W.J., Viergever M.A. : Fast quantification of abdobinal aortic aneurysms from CTA volumes. MICCAI, Cambridge MA (USA), 138-145.

1999

[22] Chung A.C.S., Noble J.A. : Statistical 3D vessel segmentation using a Rician distribution. MICCAI, Cambridge (UK), (Springer), 82-89.
[23] Frangi A.F., Niessen W.J. et al. : Quantitation of vessel morphology from 3D MRA. MICCAI, Cambridge (UK), (Springer) 358-367.
[24] Frangi A.F., Niessen W.J. et al. : Model-based quantitation of 3D Magnetic Resonance Angiographic images. IEEE Trans. MI, 18(10), 946-956.
[25] Hernández-Hoyos M., Orkisz M. et al. : Inertia-based vessel axis extraction and stenosis quantification in 3D MRA images. Comp. Assisted Radiol. & Surgery, Paris (F), (Elsevier), 189-193.
[26] Martinez-Pérez M.E., Hughes A.D. et al. : Retinal blood vessel segmentation by means of scale space analysis and region growing. MICCAI, Cambridge (UK), (Springer), 90-97.
[27] Parker D.L., Chapman B.E. et al. : A novel segmentation and display technique : the depth buffer segmentation (DBS) algorithm. 11th Int Workshop on Magn. Reson. Angio., Lund (S), 97.
[28] Wink O., Niessen W.J. et al. : Semi-automated quantification and segmentation of abdominal aorta aneurysms from CTA volumes. Comp. Assisted Radiol. & Surgery, Paris (F), (Elsevier), 208-212.